UC Irvine
UC Irvine Previously Published Works

Title

Histone Deacetylase SIRT1 Controls Proliferation, Circadian Rhythm, and Lipid Metabolism during Liver Regeneration in Mice*

Permalink

Journal

ISSN

Authors

Bellet, Marina Maria
Masri, Selma
Astarita, Giuseppe
et al.

Publication Date

DOI

Copyright Information

Peer reviewed

Histone Deacetylase SIRT1 Controls Proliferation, Circadian Rhythm, and Lipid Metabolism during Liver Regeneration in Mice[*]

Marina Maria Bellet[‡1], **Selma Masri**[§], **Giuseppe Astarita**[¶‖], **Paolo Sassone-Corsi**[§], **Maria Agnese Della Fazia**[‡], **and Giuseppe Servillo**[‡2]

From the ‡*Department of Experimental Medicine, University of Perugia, 06132 Perugia, Italy,* §*Center for Epigenetics and Metabolism, Department of Biological Chemistry, University of California, Irvine, Irvine, California 92697,* ¶*Health Sciences, Waters Corporation, Milford, Massachusetts 01757, and* ‖*Department of Biochemistry and Molecular and Cellular Biology, Georgetown University, Washington DC 20057*

Liver regeneration offers a distinctive opportunity to study cell proliferation *in vivo*. Mammalian silent information regulator 1 (SIRT1), a NAD^+-dependent histone deacetylase, is an important regulator of various cellular processes, including proliferation, metabolism, and circadian rhythms. In the liver, SIRT1 coordinates the circadian oscillation of clock-controlled genes, including genes that encode enzymes involved in metabolic pathways. We performed partial hepatectomy in WT and liver-specific Sirt1-deficient mice and analyzed the expression of cell cycle regulators in liver samples taken at different times during the regenerative process, by real time PCR, Western blotting analysis, and immunohistochemistry. Lipidomic analysis was performed in the same samples by MS/HPLC. We showed that G_1/S progression was significantly affected by absence of SIRT1 in the liver, as well as circadian gene expression. This was associated to lipid accumulation due to defective fatty acid beta-oxidation. Our study revealed for the first time the importance of SIRT1 in the regulation of hepatocellular proliferation, circadian rhythms, and lipid metabolism during liver regeneration in mice. These results represent an additional step toward the characterization of SIRT1 function in the liver.

In response to various types of injuries, the liver rapidly regenerates to restore its original size and function. Liver regeneration following partial hepatectomy (PH)[3] is one of the most effective models for studying hepatocellular proliferation (1), and involves a complex interplay of signaling events, many of which still need to be elucidated (2). After resection of two-thirds of the liver mass in rodents, according to the Higgins and Anderson procedure (3), residual hepatocytes rapidly enter the cell cycle and perform about two cycles of cell division. Many factors, including hormones, cytokines, growth factors, and their coupled signal transduction pathways contribute to initiating and promoting progression of hepatocytes through the G_1/S phase, and subsequent cell division (1). Several groups of genes are activated in a distinct temporal manner, thus maintaining the efficiency of the regenerative process (4–8). Moreover, specific metabolic changes are associated with the process of liver regeneration. In particular, a transient steatosis occurs during liver regeneration and appears to be important for proper regenerative response, though its functional significance remains poorly defined (9, 10).

Silent information regulator 1 (SIRT1), the most studied member of the mammalian sirtuin family of NAD^+-dependent histone deacetylases, is a nutrient sensor and a crucial regulator of aging in different organisms (11). SIRT1 plays a central role in the control of normal liver function in mammals, and participates in the regulation of metabolic processes including gluconeogenesis, fatty acid beta-oxidation and cholesterol flux (12). Moreover, SIRT1 has been recognized as an important regulator of circadian rhythms in the liver and brain (13–15). In the liver, SIRT1 acts by ensuring proper circadian oscillation in hepatocytes through rhythmic deacetylation of histone H3 at the promoter of clock-controlled genes (CCGs), as well as deacetylation of the circadian components BMAL1 and PER2 (13, 15). SIRT1 activity itself oscillates in a circadian manner, following the availability of its coenzyme NAD^+, that is rhythmic over the day/night cycle (16, 17). Genetic or pharmacological modulation of SIRT1 expression and/or activity in the liver resulted in altered hepatic circadian gene expression and metabolism (18, 19), pointing to its importance in maintaining proper circadian regulation of metabolic and epigenetic processes in the liver.

Direct molecular links between the circadian clock and cellular proliferation have been established (20). The circadian machinery regulates the rhythmic expression of a number of key regulators of cell cycle progression (Wee-1, c-myc, Cyclin D1) and DNA-damage response (Gadd45a, MDM2, XPA) (21–23). Furthermore, liver regeneration is impaired in arrhythmic

[3] The abbreviations used are: PH, partial hepatectomy; SIRT1, silent information regulator 1; CCG, clock-controlled gene; LKO, liver-specific knock-out; CDK, cyclin-dependent kinase; NL, normal liver; ZT, zeitgeber time; H&E, hematoxylin and eosin; TAG, triacylglycerides; NEFA, non-esterified fatty acids; SFA, saturated FA, MUFA, mono-unsaturated FA; PUFA, poly-unsaturated FA.

Cry1/2 knock-out mice (24). In this study we performed PH to induce hepatic regeneration in wild-type (WT) and liver-specific SIRT1$^{\Delta ex4}$ mice (Sirt1 LKO), to assess the role of SIRT1 in governing cell cycle progression and metabolic changes during liver regeneration. Moreover, we tested the hypothesis that the circadian function of SIRT1 might play a role in the regulation of hepatocyte proliferation. We conclude that liver-specific deletion of SIRT1 resulted in significant alterations in circadian function linked to hepatocyte progression through the cell cycle and lipid metabolism after PH.

Results

Cell Cycle Progression Is Impaired in Sirt1 LKO Regenerating Livers—PH was performed in WT and Sirt1 LKO mice and regenerating livers were collected at different times to analyze cell-cycle progression. In the livers of WT mice, as was previously described (1), *Ccnd1* (Cyclin D1) and *Ccne1* (Cyclin E1) gene expression profiles were significantly elevated at 36 h following PH, followed by a second increase observed at 48 h for *Ccnd1*. In the livers of Sirt1 LKO mice, *Ccnd1* was up-regulated earlier, but levels of both peaks of mRNA expression were markedly reduced, indicating an impaired exit from G_0. Similarly, the peak in *Ccne1* expression was abolished in Sirt1 LKO mice (Fig. 1*A*). *Ccna2* (Cyclin A2) peaked between 38 and 48 h in both WT and Sirt1 LKO mice, but the levels were reduced and the expression prolonged until 60 h in conditional mice. Levels of *Cdk4*, the cyclin-dependent kinase (CDK) important for the progression through the G_1 phase, were also slightly reduced in regenerating livers from Sirt1 conditional KO mice, while the expression of other factors (*Ccnd3*) was not affected (Fig. 1*A*).

Because regulation of cyclin stability occurs largely post-transcriptionally, we also analyzed protein expression levels in the same livers. Western blotting (WB) analysis confirmed that both Cyclin D1 and Cyclin A2 expression was reduced during the first G_1/S phase following PH in the liver from Sirt1 LKO mice, while the second peak of expression, normally occurring at 60 h after PH and corresponding to the second round of DNA synthesis, was maintained and even enhanced compared with WT mice. Similarly, Cyclin E1 and Cdk4 protein expression peaked at 36 h following PH in WT mice, while the peak was strongly reduced in LKO mice (Fig. 1*B*). The second peak of expression was enhanced for both Cyclin E1 and Cdk4, as confirmed by densitometric analysis (Fig. 1*C*).

Taken together, these results reveal a defect in G_1/S progression in the liver of Sirt1 LKO mice during the first peak of cell division, which is apparently compensated during the second peak.

Delayed Mitosis in Regenerating Livers of Sirt1 LKO Mice—We next examined the progression through the G_2/M phase after liver regeneration in WT and Sirt1 LKO mice. With this purpose, we analyzed mRNA expression of central regulators of the G_2/M transition. While no differences were found in the expression of *Cdk1*, a significant reduction in the level of expression of *Ccnb1* (Cyclin B1), *Ccnb2* (Cyclin B2), and *Wee1* was observed in LKO mice by Q-PCR (Fig. 2*A*), thus confirming the impaired cell cycle progression in the absence of SIRT1.

We also determined the phosphorylation of Serine 10 of histone H3 (p-S10H3), a key step in chromosome remodelling during cell division. Furthermore, p-S10H3 is a marker that differentiates between G_2-phase and mitotic cells. In both WT and Sirt1 LKO mice, WB and immunohistochemistry analysis showed a peak in H3 phosphorylation at 48 h following PH, corresponding to the first mitotic wave (Fig. 2, *B* and *C*). However, in WT mice the majority of positive cells were in M phase, in Sirt1 LKO mice the number of mitotic nuclei was reduced, and many cells remained in G_2, thus suggesting a delayed entry into mitosis in LKO mice (Fig. 2, *C* and *D*). Moreover, a significant increase in the number of nuclei in G_2 was present in Sirt1 LKO mice at 60 h following PH (Fig. 2, *C* and *E*), confirming the enhanced progression through the cell cycle observed during the second wave of cell division, possibly as a compensatory mechanism. Overall, these findings point to a delay in the progression of hepatocytes through the cell cycle in the absence of Sirt1.

Cell Cycle Regulator p21$^{Waf/Cip1}$ Is Down-regulated in Sirt1 LKO Mice—The activity of cyclin/CDK complexes is negatively regulated by cyclin kinase inhibitors, including p21$^{Waf/Cip1}$ and p27^{Kip1} (25). We studied p21$^{Waf/Cip1}$ and p27^{Kip1} mRNA expression levels during liver regeneration in WT and Sirt1 LKO mice, to understand whether an overstated inhibitory response could account for the reduced expression of markers of G_1/S proliferation. As previously observed (25), the p21$^{Waf/Cip1}$ gene *Cdkn1a* is not detected in normal liver (NL) of WT mice, while is markedly induced 6 h after PH, in the early G_1 phase, and again at 36 and 60 h, corresponding to the two waves of cell division (Fig. 3*A*). In LKO mice, while the first peak of p21$^{Waf/Cip1}$ mRNA expression is maintained, surprisingly its expression subsequently declines to very low levels, indicating that p21$^{Waf/Cip1}$ fails to be activated during the post-replicative phase. Instead, no change was observed in the transcription of the p27^{Kip1} gene *Cdkn1b* (Fig. 3*A*). In line with mRNA expression, we found that the induction of p21$^{Waf/Cip1}$ protein observed in WT livers at 48 h after PH was completely absent in livers from Sirt1 LKO mice (Fig. 3*B*). Since p21$^{Waf/Cip1}$ is transcriptionally regulated by p53, we monitored p53 expression levels and found that p53 protein was not induced at 36 h following PH in Sirt1 LKO, as instead occurs in WT livers (Fig. 3*B*).

All together, these data indicate that increased expression of cell cycle inhibitors p21$^{Waf/Cip1}$ and p27^{Kip1} cannot explain the delay in cell cycle progression observed in Sirt1 LKO mice. Instead, p21$^{Waf/Cip1}$ is down-regulated during the G_1/S progression in Sirt1 LKO mice, because of a reduction in p53 protein induction in these mice.

Circadian Gene Expression Is Dampened during Liver Regeneration in Sirt1 LKO Mice—Several levels of functional interplay exist between molecular components of the clock machinery and cell cycle regulators (20). Given the central role of SIRT1 in controlling proper circadian transcription in the liver (13, 15, 17–19, 26), we decided to explore the possibility that absence of SIRT1 could alter circadian gene expression during liver regeneration. In NL taken at different times of the circadian cycle (zeitgeber time, ZT), the expression of core clock genes such as *Bmal1, Cry1,* and *Per2* follows a typical circadian
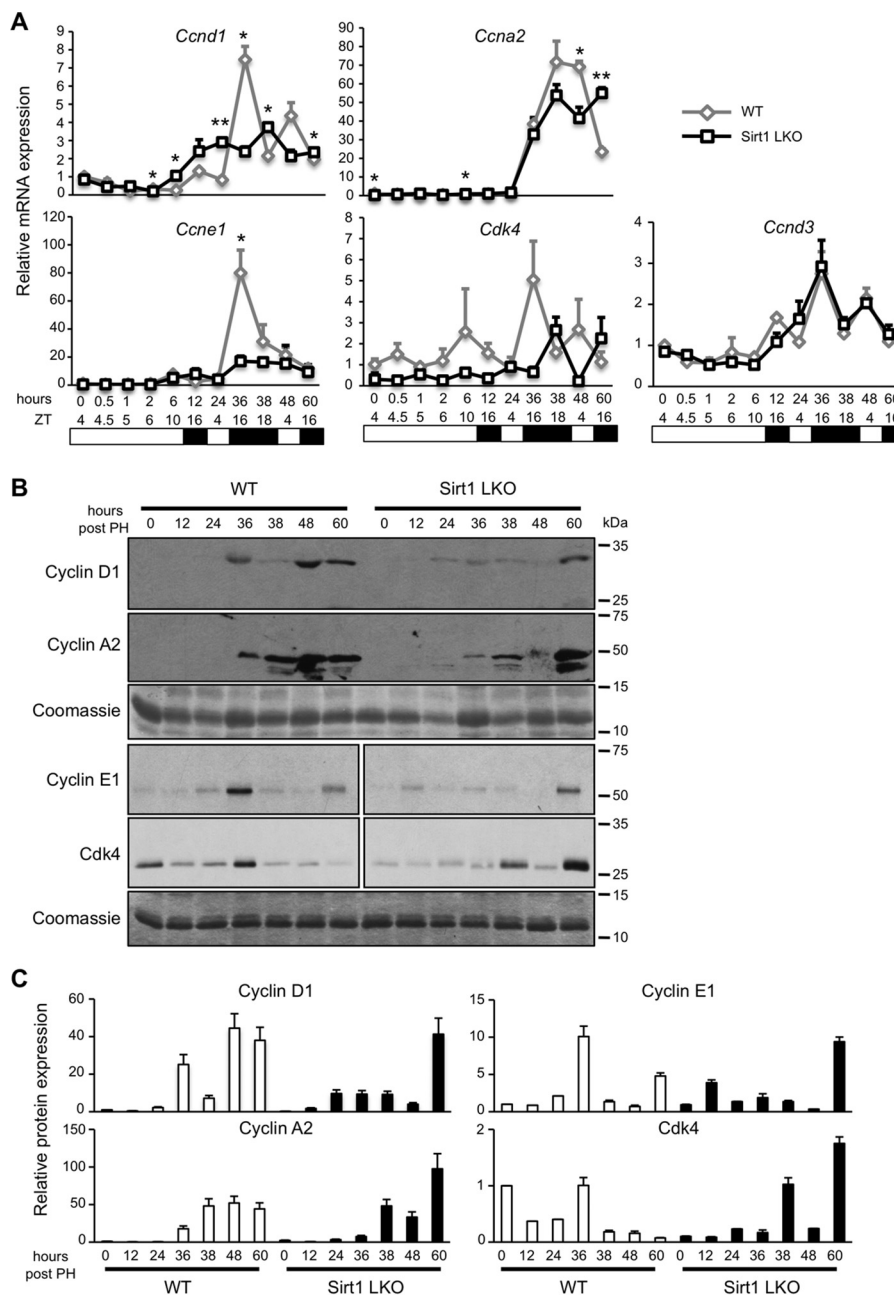
FIGURE 1. **Defective G_1/S transition during liver regeneration in Sirt1 liver KO mice.** *A*, time course of mRNA expression of different cyclins (*Ccnd1*, *Ccne1*, *Ccna2*, *Ccnd3*) and cyclin-dependent kinases (*Cdk4*) controlling G_0/G_1 and G_1/S transitions during liver regeneration at different times (hours) following partial hepatectomy (PH), in WT and Sirt1 liver-specific KO (LKO) mice. *Black* and *white bars* represent circadian light-dark phases at each specific zeitgeber times (ZT). The mRNA values are relative to those of 18S mRNA levels at each time point. Bars represent mean $\pm$ S.D. ($n = 3$–8). Significant changes are shown. *, $p < 0.05$; **, $p < 0.01$. *B*, protein expression of Cyclin D1, Cyclin A2, Cyclin E1, and Cdk4 in regenerating livers from WT and Sirt1 LKO mice, evaluated by Western blotting analysis (WB). Coomassie Blue staining was used as loading control. Representative images are shown. *C*, densitometric analysis of immunoblotting signals of Fig. 1*B*. Values were normalized to the level of histones staining with Coomassie Blue. Bars represent means $\pm$ S.D. ($n = 3$).

oscillation, peaking around ZT0, ZT20, and ZT16, respectively (Fig. 4*A*). Similarly, CCGs like *Nampt* and *Dbp* show a strong circadian oscillation in the liver (Fig. 4*A*), as previously observed (18). Absence of *Sirt1* altered the expression of circadian genes in NL, in most of the cases (*Per2*, *Nampt*, *Dbp*) by producing an enhanced oscillation (Fig. 4*A*) (15, 18, 19).

In line with previous findings (24), the oscillation of circadian genes was maintained during liver regeneration, as demonstrated by their peak of expression at specific time points following PH, corresponding to the ZT of their maximum peak in

NL (Fig. 4*B*). The only exception was *Dbp*, the expression of which was down-regulated at the beginning of the regenerative process (Fig. 4*B*). We also observed that *Bmal1* mRNA showed an additional peak of expression at 36 h following PH in WT livers, corresponding to ZT16, that does not coincide with its daily zenith and thus represents an induction associated to the regenerative process (Fig. 4*B*), suggesting an active role of BMAL1 during hepatocyte proliferation. Surprisingly, in the liver from Sirt1 LKO mice, the expression level of both *Bmal1* and *Cry1* was strongly down-regulated. Similarly, but to a lesser
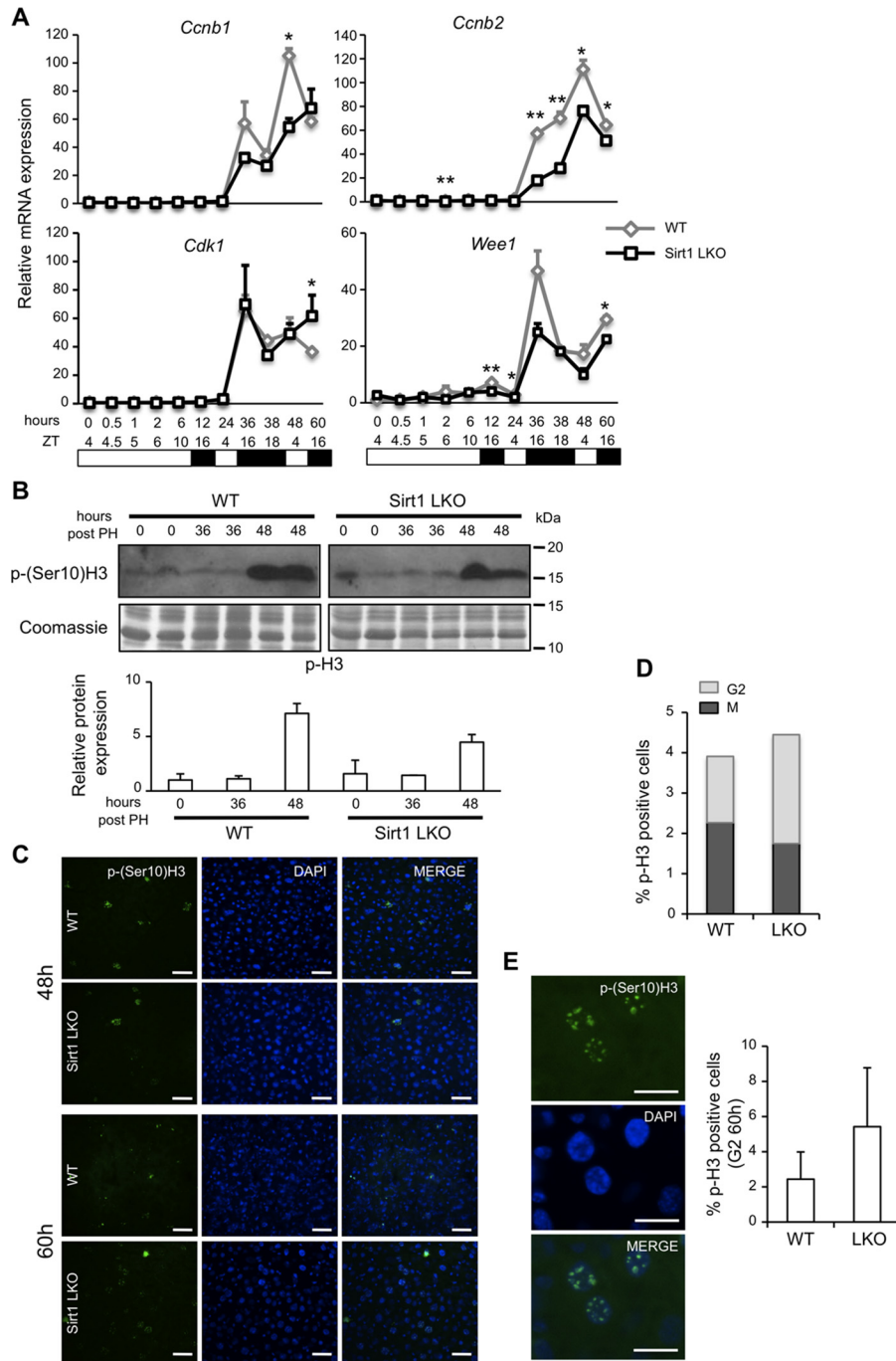
FIGURE 2. **Mitosis is slightly delayed in Sirt1 KO regenerating livers.** *A*, time course of mRNA expression of *Ccnb1*, *Ccnb2*, *Cdk1*, and *Wee1* controlling G_2/M transitions during liver regeneration at different times following PH, in WT and Sirt1 LKO mice. *Black* and *white bars* represent circadian light-dark phases at each specific ZT. The mRNA values are relative to those of 18S mRNA levels at each time point. Bars represent mean ± S.D. (*n* = 3–8). Significant changes are shown. *, $p < 0.05$; **, $p < 0.01$. *B*, Western blotting analysis of p-(Ser10)H3 protein expression level in livers at different times (hours) following PH. Coomassie Blue staining was used as loading control. Representative images are shown. Densitometric analysis of immunoblotting signals was shown. Values were normalized to the level of histones staining with Coomassie Blue. Bars represent means ± S.D. (*n* = 3). *C*, immunolocalization of phospho-H3 in livers from WT and Sirt1 LKO mice at 48 and 60 h after PH, analyzed by using p-(Ser10)H3 antibody. DAPI was used for labeling nuclei (*blue*). Representative images (200× magnification) are shown. Bars, 10 μM. *D*, percentage of p-H3-positive hepatocytes observed at 48 h after PH. (400× magnification, *n* = 15 fields of observation from at least 3 mice). *E*, representative image of p-(Ser10)H3 positive nuclei in G2 phase at 60 h after PH in livers from WT and Sirt1 LKO mice, analyzed by using p-(Ser10)H3 antibody. DAPI was used for labeling nuclei (*blue*). Bars, 5 μM. *Right*, percentage of p-H3-positive hepatocytes in G2 phase observed at 60 h after PH. Bars represent mean ± S.D. (*n* = 15 fields of observation from at least three mice).

extent, the expression of *Per2* and *Nampt* was dampened at 36 h after PH, but the oscillation was maintained (Fig. 4*B*). WB analysis of WT and KO livers using BMAL1 and CRY1 specific antibodies indicated that their reduction in mRNA levels corresponded to very low levels of protein in livers from Sirt1 LKO

mice (Fig. 4*C*). These results suggested that SIRT1 is essential in maintaining proper circadian expression of core clock genes in regenerating livers.

Since many cell cycle regulators are known to be transcribed in a circadian manner, we wondered whether their circadian
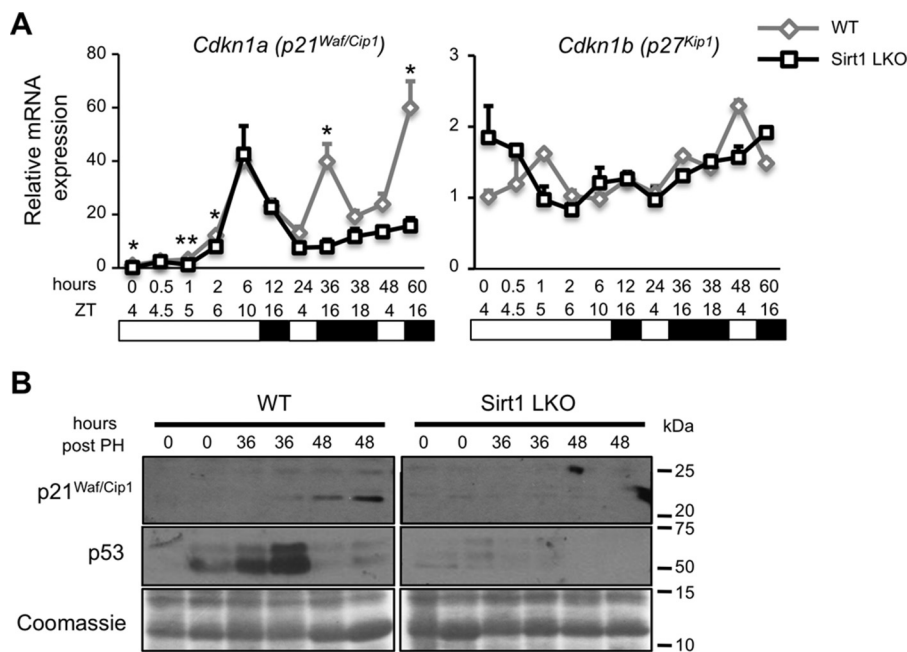
FIGURE 3. **The p53/p21^Waf/Cip1 axis is down-regulated in Sirt1 LKO mice during liver regeneration.** *A*, Q-PCR analysis of *Cdkn1a* (p21^Waf/Cip1) and *Cdkn1b* (p27^Kip1) from RNA samples prepared from livers of WT and Sirt1 LKO mice at different times after PH. *Black* and *white bars* represent circadian light-dark phases at each specific ZT. The mRNA values are relative to those of 18S mRNA levels at each time point. Bars represent mean ± S.D. ($n = 3$–8). Significant changes are shown. *, $p < 0.05$; **, $p < 0.01$. *B*, protein expression of p21^Waf/Cip1 and p53 in normal livers (0 h) and regenerating livers at 36 and 48 h after PH, from WT and Sirt1 LKO mice, evaluated by WB. Coomassie Blue staining was used as loading control. Representative images are shown.

expression could be defective in normal non-regenerating livers of Sirt1 LKO mice. Q-PCR analysis of mRNA expression of cyclins and CDKs in NL at six different times of the circadian cycle indicates that while some genes follow a clear circadian rhythm of expression (*Cnkn1a, Ccne1*), others are not oscillating (*Cdk4, Ccna2*), with no relevant differences between WT and Sirt1 LKO mice (Fig. 4*D*). This reveals that the presence of SIRT1 is dispensable to maintain proper circadian expression of these genes in NL, while it is essential during liver regeneration after PH.

Sirt1 LKO Mice Display Enhanced Liver Steatosis during Liver Regeneration—In addition to the investigation of circadian clock dysfunction as a cause of cell cycle deregulation, we decided to explore whether metabolic changes normally occurring during liver regeneration were affected by the absence of SIRT1, and if this could in turn alter cell cycle progression. Indeed, circadian rhythms play a pivotal role in the regulation of metabolic processes in quiescent liver.

Liver regeneration following PH is typically associated with an induction of fat synthesis, which is considered to be an essential metabolic response within the regenerating liver (27). In liver sections stained with hematoxylin and eosin (H&E), we observed a transient steatosis in WT livers starting from 24 h until 48 h after PH. In Sirt1 LKO mice the level of steatosis was markedly increased at almost all time points analyzed (Fig. 5*A*). No lipid accumulation was detected in NL of WT and Sirt1 LKO mice.

We then used a lipidomics approach to analyze levels and lipid composition in WT and Sirt1 LKO mice. We used liquid chromatography/mass spectrometry (LC/MS) to survey samples of NL and livers at 36 and 48 h after PH. We found similar basal levels of triacylglycerides (TAG), cholesterol esters and

non-esterified fatty acids (NEFA) (Fig. 5*B*) in NL from WT and Sirt1 LKO mice, as previously reported (28). In line with this result, no difference in body weight and food intake was observed in these mice (Fig. 5*C*) (29). Interestingly, during liver regeneration, levels of TAG and cholesterol esters increased transiently in both WT and LKO mice at 36 h, but they were maintained at elevated levels at 48 h in LKO mice (Fig. 5*B*). Moreover, in Sirt1 LKO mice, but not in WT mice, we observed increased levels of total NEFA at 36 and 48 h following PH (Fig. 5*B*). NEFA vary in length and saturation and we observed a general trend characterized by increased levels of both saturated FA (SFA) and mono- and poly-unsaturated FA (MUFA and PUFA) at 36 h following PH in Sirt1 LKO mice (Fig. 6, *A* and *B*). At 48 h there was a specific increase only in unsaturated FA, both in long chain and very long chain classes (Fig. 6, *A* and *B*), as confirmed by the desaturation index that was increased in livers from Sirt1 LKO mice (Fig. 6*C*). Taken together, these data reveal abnormally increased lipid accumulation and alterations in lipid composition in Sirt1 LKO mice during liver regeneration following PH.

Reduced NEFA Oxidation in Sirt1 KO Regenerating Livers— The increased lipid accumulation observed in Sirt1 KO liver following PH may be caused by an increased FA synthesis, as SIRT1 controls the activity of SREBP-1c, the main regulator of FA synthesis and elongation (30), through deacetylation and inhibition of its transcriptional activity. To validate this hypothesis, gene expression of SREBP target genes was measured by Q-PCR. In Sirt1 LKO mice, we observed significantly higher levels of SREBP target genes controlling NEFA synthesis (*Fasn, AceCS1*), desaturation (*Scd1*) and elongation (*Elovl2*) in NL. Instead, no differences were found in regenerating livers between WT and Sirt1 LKO mice, with the exception of *Scd1*,
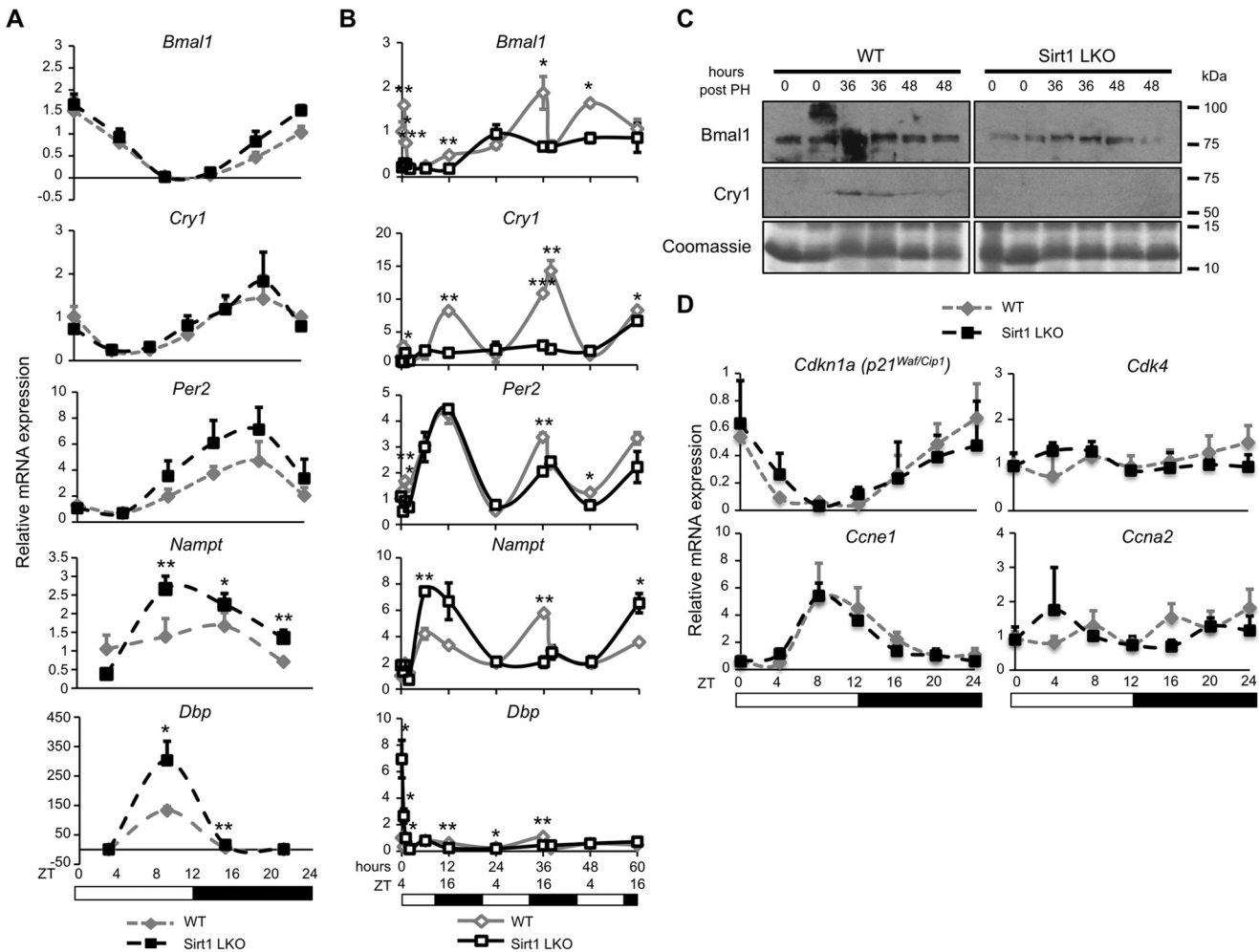
FIGURE 4. **Defects in circadian gene expression in Sirt1 KO regenerating livers.** *A*, Q-PCR analysis of genes *Bmal1*, *Cry1*, *Per2*, *Nampt*, and *Dbp* from RNA samples prepared from livers of WT and Sirt1 LKO mice at different times through the circadian cycle (ZT). *Black* and *white bars* represent circadian light-dark phases. The mRNA values are relative to those of *18S* mRNA levels at each time point. Bars represent mean ± S.D. ($n = 5$). Significant changes are shown. *, $p < 0.05$; **, $p < 0.01$. *B*, time course of mRNA expression of *Bmal1*, *Cry1*, *Per2*, *Nampt*, and *Dbp* during liver regeneration at different times (hours) following PH, in WT and Sirt1 LKO mice. *Black* and *white bars* represent circadian light-dark phases at each specific ZT. The mRNA values are relative to those of 18S mRNA levels at each time point. Bars represent mean ± S.D. ($n = 3$–8). Significant changes are shown. *, $p < 0.05$; **, $p < 0.01$; ***, $p < 0.001$. *C*, protein expression of Bmal1 and Cry1 in regenerating livers from WT and Sirt1 LKO mice, evaluated by WB. Coomassie Blue staining was used as loading control. Representative images are shown. *D*, Q-PCR analysis of genes *Cdkn1a*, *Ccne1*, *Cdk4*, and *Ccna2* from RNA samples prepared from livers of WT and Sirt1 LKO mice at different times through the circadian cycle (ZT). *Black* and *white bars* represent circadian light-dark phases. The mRNA values are relative to those of 18S mRNA levels at each time point. Bars represent mean ± S.D. ($n = 3$).

whose expression at 48 h after PH was higher in Sirt1 LKO mice (Fig. 7*A*), thus explaining the prevalent increase in polyunsaturated FA at this time point. Furthermore, the level of acetylation of SREBP-1c was evaluated in SIRT1 WT and LKO regenerating livers. In line with gene expression results, we found similar levels of acetylation of SREBP-1c in both genotypes, thus suggesting identical activation after PH (Fig. 7*B*).

Alternatively, a reduction of FA beta-oxidation might explain the accumulation of fat in Sirt1 KO livers during hepatic regeneration. Indeed, under high-fat diet Sirt1 LKO mice accumulate an excessive amount of fat due to a defect in FA beta-oxidation dependent on PPARα (28), a nuclear receptor whose expression and transcriptional activity is directly regulated by the circadian system (31). For this reason, we asked whether this defect could also be responsible for the high grade of steatosis observed in these mice following PH. Indeed, the expression of fatty acid ω-hydroxylase genes *Cyp4a10* and *Cyp4a14*, PPARα target genes, as well as the expression of other genes

involved in NEFA oxidation, such as *Acox1* and *Acadm,* was strongly induced in WT mice after PH. This induction in gene expression was significantly diminished at 48 h after PH in Sirt1 LKO mice (Fig. 7*A*). Moreover, transcription of the gene encoding the enzyme mtGPAT, that controls the esterification of NEFA to glycerol for the synthesis of TAG, was increased in Sirt1 LKO mice compared with WT (Fig. 7*A*), suggesting that the increased levels of liver NEFA in Sirt1 LKO mice is responsible of the increased TAG accumulation after PH.

To finally demonstrate that a defective activation of PPARα is directly responsible of the down-regulation of its target genes, we evaluated its level of expression in normal and regenerating livers from WT and SIRT1 LKO mice. Importantly, we found a strong up-regulation of PPARα protein expression in WT mice during liver regeneration, while the induction was completely abolished in SIRT1 KO liver (Fig. 7*C*). Therefore, a defect in FA beta-oxidation appears to be the main mechanism responsible for lipid accumulation in SIRT1 KO mice following
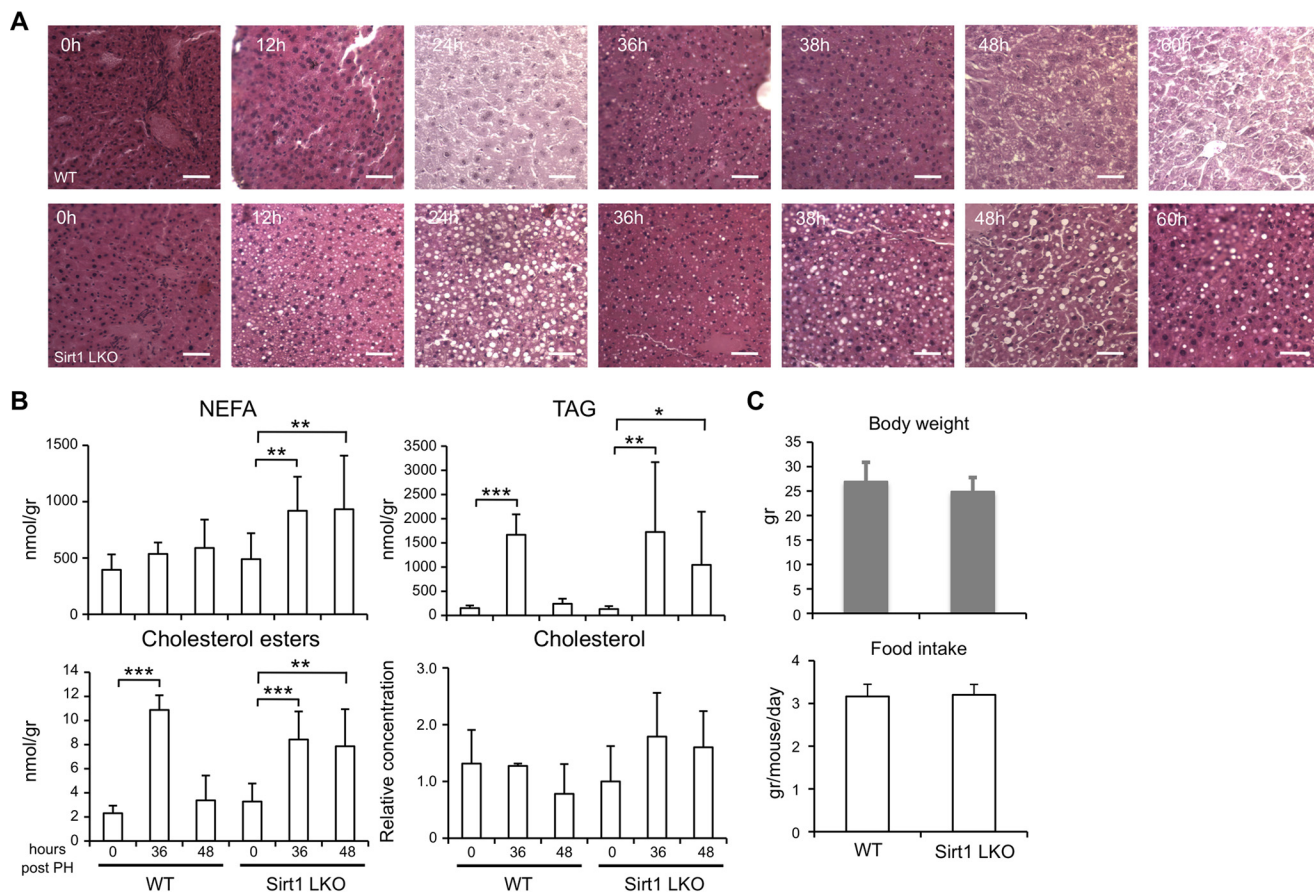
FIGURE 5. **Lipid accumulation in Sirt1 KO regenerating livers.** *A*, H&E staining on liver sections of WT and Sirt1 LKO mice at indicated times following PH. Representative images (200× magnification) are shown. Bars, 10 μM. *B*, levels of NEFA, TAG, cholesterol esters, and cholesterol in livers from WT and Sirt1 LKO mice at indicated times after PH, measured by LC-MS analysis. Bars represent mean ± S.D. (*n* = 3–8). Significant changes are shown. *, $p < 0.05$; **, $p < 0.01$; ***, $p < 0.001$. *C, top*, body weight (grams, gr) of 3-month-old Sirt1 WT and LKO mice. *Bottom*, food pellet grams consumed per day from Sirt1 WT and LKO mice.

PH, due to a defective induction of PPARα during liver regeneration in SIRT1 LKO mice.

In conclusion, these results reveal that SIRT1 regulates several related aspects of the process of liver regeneration in mice, and point to a circadian defect in proliferating hepatocytes due to absence of SIRT1, that may explain the altered timing of cell cycle progression and fat metabolism in regenerating liver (Fig. 8).

Discussion

By controlling metabolism in response to low nutrient availability, SIRT1 contributes to the maintenance of energy homeostasis. In the liver, SIRT1 is an important regulator of metabolic processes such as gluconeogenesis, NEFA oxidation, mitochondrial activity and cholesterol flux, which occur in response to an intracellular rise in the NAD$^+$/NADH ratio when energy supplies are low. Moreover, SIRT1 is a central component of the circadian clock machinery and its absence is associated with alterations in circadian gene expression in NL. To further examine the function of SIRT1 in the liver, liver-specific Sirt1 knock-out mice were generated (29). Although these mice are phenotypically normal under a chow diet, hepatic steatosis and inflammation was observed in response to high-fat feeding (28).

We demonstrated that SIRT1 might have additional functions in the liver following PH, a paradigm that extends beyond nutritional challenge. We observed a transient but relevant defect in the progression of hepatocytes from G_0/G_1 to S phase in Sirt1 LKO mice, characterized by deregulation of the expression of cyclins and CDKs controlling G_1/S phase, and to a minor extent, those controlling the G_2/M phase. This defect seems to be compensated for during the second wave of cell division, when an increase in the number of pre-mitotic cells was observed as measured by p-H3 positive nuclei. In line with our results, a recent study showed that livers from old mice, expressing low levels of SIRT1, as well as livers in which *Sirt1* gene expression was silenced, show defective regeneration (32). Moreover, it has been shown that SIRT1 overexpression is associated with impaired hepatocyte proliferation and increased mortality caused by liver injury due to bile acid accumulation (33), thus suggesting that both deficiency or exaggerated SIRT1 activity has negative effects on proliferation of liver cells. Our experiments also demonstrated that the intrinsic circadian clock is intact in proliferating liver cells from WT mice, while is disrupted in LKO mice, thus revealing the importance of SIRT1 circadian function in maintaining the correct timing and progression through the cell cycle.

The factors controlling cell proliferation and cell cycle arrest that are preferential targets of SIRT1 are numerous. SIRT1 deacetylates the tumor suppressor p53 (34), which inhibits p53 target gene transcription, including the cell cycle inhibitor p21.
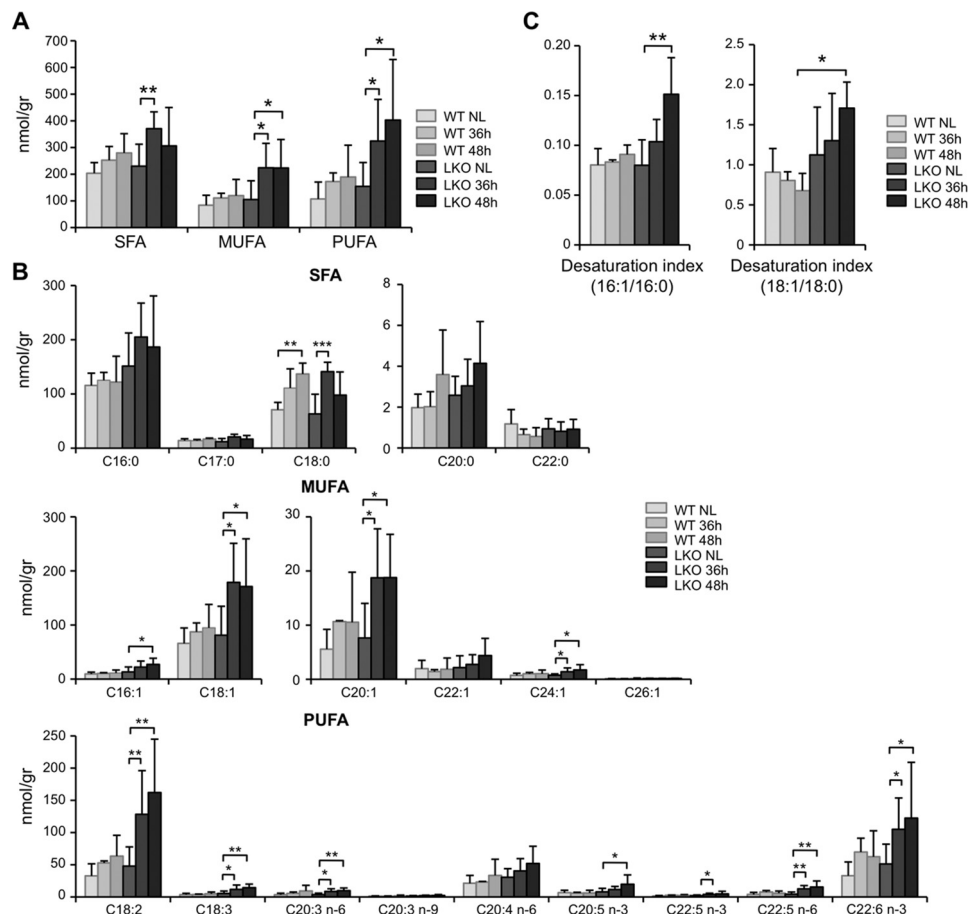
FIGURE 6. **Regulation of non-esterified fatty acids (NEFA) metabolism in Sirt1 KO regenerating livers.** *A*, LC-MS analysis of NEFA levels in livers from WT and Sirt1 LKO mice at indicated times after PH. *SFA*, saturated fatty acids; *MUFA*, monounsaturated fatty acids; *PUFA*, polyunsaturated fatty acids. Bars represent mean ± S.D. ($n = 3–8$). Significant changes are shown. *, $p < 0.05$; **, $p < 0.01$. *B*, LC-MS analysis of NEFA composition is shown at indicated times after PH. *SFA*, saturated fatty acids; *MUFA*, monounsaturated fatty acids; *PUFA*, polyunsaturated fatty acids. Bars represent mean ± S.D. ($n = 3–8$). Significant changes are shown. *, $p < 0.05$; **, $p < 0.01$; ***, $p < 0.001$. *C*, desaturation index in livers from WT and Sirt1 LKO mice at indicated times after PH. 16:1/16:0 and 18:1/18:0 NEFA ratio are shown. Bars represent mean ± S.D. ($n = 3–8$). Significant changes are shown. *, $p < 0.05$; **, $p < 0.01$.

However, the repression of both p53 protein induction and *p21* mRNA expression observed in Sirt1 LKO mice during liver regeneration suggests that SIRT1 regulation of p53 activity might not play a critical role in controlling hepatocyte proliferation during liver regeneration in these mice. Further studies will be necessary to understand the specific mechanism of how SIRT1 controls hepatocyte cell cycle progression.

The early regenerating liver transiently accumulates large amounts of triglycerides, that are used as substrates for energy production and membrane synthesis (35). Although the molecular mechanism that regulates this event is poorly defined, hepatocellular fat accumulation seems to be essential for normal liver regeneration, as its suppression is associated with impaired hepatocellular proliferation following PH (35). On the other hand, chronic hepatic steatosis is also associated with impaired regeneration, thus confirming the importance of a fine-tuned regulation of lipid metabolism for liver regeneration. Using a lipidomic strategy, we observed abnormally high accumulation of TAGs, cholesterol esters and NEFAs in regenerating livers of Sirt1 LKO mice, thus suggesting an important role of SIRT1 in regulating the proper balance of fat production during hepatocyte proliferation. Moreover, an alteration in lipid composition was observed, with increased expression of

unsaturated FA that could play an important role in the control of signal transduction pathways, enzymatic activity and cellular regeneration (36).

SIRT1 regulates lipid homeostasis in the liver, through deacetylation and activation of target proteins, including SREBP-1c, the main regulator of FA synthesis and elongation (30), and PPARα, a nuclear receptor that controls fatty acid β-oxidation in response to nutrient availability (28). Interestingly, absence of PPARα caused delayed liver regeneration in mice (37). We observed that the expression of PPARα target genes controlling NEFA oxidation was down-regulated in regenerating liver in Sirt1 LKO mice, and this was a consequence of a marked reduction of PPARα protein expression in those livers, thus revealing the mechanism responsible for the increased fat content in the absence of SIRT1. Instead, we observed no change in the acetylation status of SREBP-1c in Sirt1 KO regenerating livers compared with WT. Consequently, we did not measure an increased transcription of enzymes controlling NEFA synthesis in regenerating liver, but only in NL of Sirt1 LKO mice, although the levels of NEFA were not augmented in basal conditions. Interestingly, among the regulators of NEFA synthesis that was up-regulated in Sirt1 LKO mice was acetyl-CoA synthetase (AceCS1), an enzyme
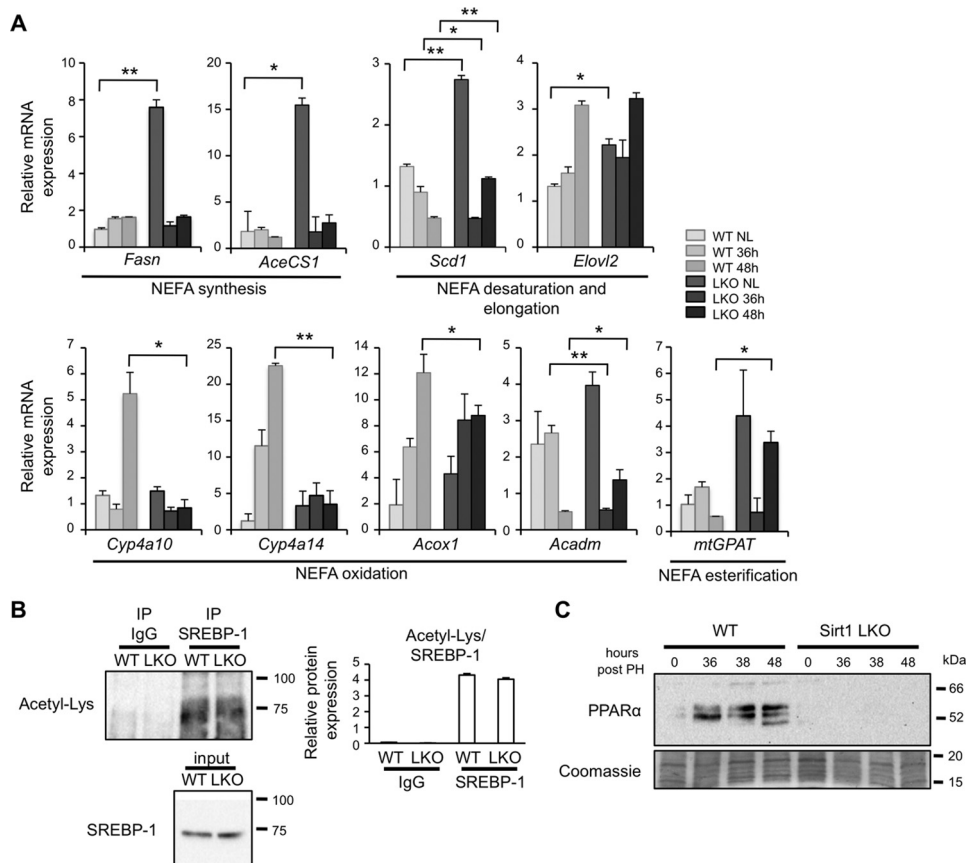
FIGURE 7. **Analysis of SREBP-1c and PPARα pathway in Sirt1 KO regenerating livers.** *A*, Q-PCR analysis of genes involved in NEFA synthesis, NEFA desaturation and elongation, NEFA oxidation and NEFA esterification from RNA samples prepared from livers of WT and Sirt1 LKO mice at the indicated times after PH. The mRNA values are relative to those of *18S* mRNA levels at each time point. Bars represent mean ± S.D. (*n* = 3–8). Significant changes are shown. *, $p < 0.05$; **, $p < 0.01$. *B*, lysates from regenerating livers at 38 h following PH were immunoprecipitated with anti-SREBP-1 antibody or rabbit IgG and immunoblotted with anti-acetylated lysine antibody. *Lower panel* shows the expression of SREBP-1 in total liver lysates as an input. *Right*, densitometric analysis of immunoblotting signals was shown. *C*, Western blotting analysis of PPARα expression in regenerating liver extracts from WT and Sirt1 LKO mice. Coomassie Blue staining was used as loading control. Representative images are shown.

controlling the availability of acetyl-CoA in the cell, which is regulated by SIRT1 through circadian deacetylation and activation (38, 39). As a result, both NEFA synthesis and elongation change in a cyclic manner (39).

Here we hypothesized that additional liver functions might be controlled by SIRT1 circadian activity. Future studies will shed light on the mechanism of how the circadian function of SIRT1 modulates the progression of hepatocytes through the cell cycle and the metabolic response of the liver during regeneration. Also, additional studies are needed to better understanding the role of SIRT1 in the proliferative process of both normal and cancer cells, with specific relevance to hepatocellular carcinoma.

Experimental Procedures

Animals—All experiments involving vertebrates were performed under a protocol approved by the Institutional Animal Care and Use Committee (IACUC) at the University of California, Irvine. WT and liver specific Sirt1$^{\Delta ex4}$ mice were previously described (29). All experiments were performed using 12–15-week-old mice housed under 12 h light/dark cycles in a temperature-controlled room, with food and water provided *ad libitum*. Liver resection of the left lateral and median lobes was performed according to the Higgins and Anderson's procedure,

between 8 and 12 am, after induction of deep anesthesia with isoflurane, by exerting a classical sub-xiphoid incision which allows extrusion, extra-abdominal ligation of the lobes, and removal of 2/3 of the liver. After the surgical procedure, animals were placed in a warmed cage to recover from surgery. Mice were sacrificed at the indicated times after PH. Regenerating livers were immediately processed for RNA and protein extraction, or frozen in liquid nitrogen and stored at −80 °C for further processing.

Reagents and Antibodies—All reagents used for HPLC-MS were from Sigma-Aldrich. Antibodies against Cyclin D1 (2926), Cyclin A2 (4656), Cyclin E1 (4129), Cdk4 (2906), p21$^{Waf/Cip}$ (2946), Acetylated-Lysine (9441) were from Cell Signaling Technology. Antibodies against p53 (sc-393031), Cry1 (sc-5953), Srebp-1 (sc-8984), PPARα (sc-398394) were from Santa Cruz Biotechnology; anti-Bmal1 (ab3350) was from Abcam; anti-Gapdh (G8795) was from Sigma-Aldrich; anti-p(Ser10)H3 (06-570) was from Millipore.

RNA Extraction and Quantitative PCR (Q-PCR)—For gene expression analysis by Q-PCR, total RNA was isolated with TRIzol Reagent (Invitrogen) and processed according to the instructions of the manufacturer. Next, 1 μg of RNA from each sample was retrotranscribed (IScript RT Supermix, Bio-Rad
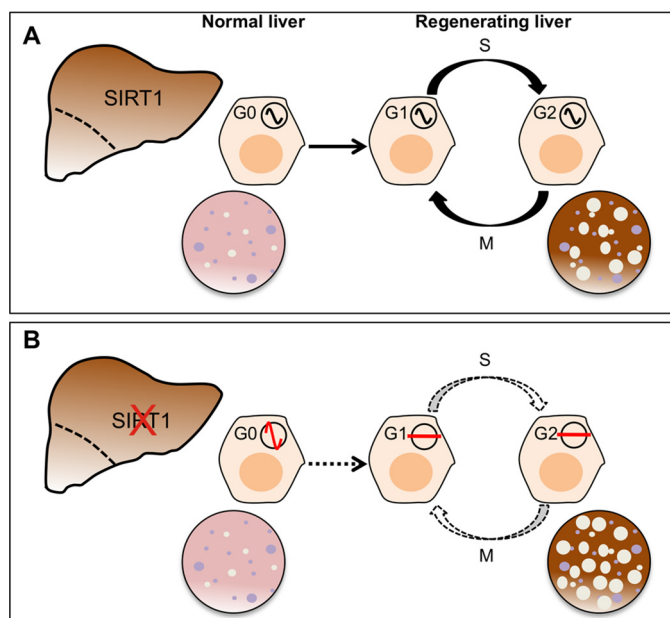
FIGURE 8. **Schematic representation of changes during liver regeneration in WT and Sirt1 LKO mice.** *A*, in WT mice, SIRT1 contributes to the maintenance of a proper circadian expression of clock genes and metabolic genes both in quiescent hepatocytes and during liver regeneration. *B*, in absence of SIRT1, mild changes occur in normal liver. Instead, when hepatocytes are induced to proliferate following PH, they are struggling to proceed through the cell cycle, accumulates lipids and circadian rhythm is dampened.

Laboratories), and 4-fold diluted cDNA was used for each real time reaction. For 20 μl of PCR, 50 ng of cDNA was mixed with primers to a final concentration of 150 nM and 10 μl of Brilliant SYBR® Green QPCR Master Mix (Agilent Technologies) and ROX as reference dye. The reaction was first incubated at 95 °C for 3 min, followed by 40 cycles at 95 °C for 30 s and 60 °C for 1 min. Quantitative PCR was performed by monitoring in real time the increase in fluorescence on an Mx3000P™ Real-Time PCR detector system. All values are relative to those of *18S* mRNA levels at each time point. Bars represent the mean ± S.D. ($n = 3 – 8$). Real-time PCR data were analyzed using the 2-$\Delta\Delta$Ct method to calculate the relative level of each mRNA and expressed as a ratio relative to 18S rRNA housekeeper gene.

Immunoblot Analysis—Fresh regenerated liver tissue was homogenized in Laemmli sample buffer, boiled, and sonicated. Protein extracts were normalized by SDS-PAGE followed by Coomassie Blue staining. Proteins expression was examined by Western blotting analysis. Each sample was separated in a SDS-PAGE gel and transferred to a nitrocellulose filter. Blots were incubated with the specific primary antibody in 5% fat-free milk; the membranes were then incubated with horseradish peroxidase, conjugated anti-rabbit or anti-mouse IgG antibody and signals were visualized using an ECL chemoluminescence (GE Healthcare Lifescience). Protein band intensities were quantified by densitometric analysis using Image J software.

Liver Histology and Immunohistochemistry—Fragments of normal and regenerated liver were fixed in 10% formalin and then embedded in paraffin after serial dehydration in alcohol for histology, or included in Tissue-Tek® O.C.T Compound (Optimum Cutting Temperature, SAKURA) and stored at −80 °C until use for immunohistochemistry. The paraffin embedded livers were sectioned (5 μm) and stained by H&E to study tissue structure and lipid accumulation. Frozen livers were sectioned (5 μm) and incubated with anti-p-S10H3 antibody. 4′, 6-diamidino-2-phenylindole (DAPI) was added at the final concentration of 10 ng/ml and was used for labeling of nuclei (blue). Slides were examined with a Zeiss Axioplan fluorescence microscope. The images were acquired by using a Spot-2 cooled camera (Diagnostic Instruments). Total p-S10H3-labeled hepatocytes were determined by counting positively stained cell nuclei in 15 microscope fields (200X magnification) per liver section at each experimental point.

Lipid Extractions—Frozen tissue samples were weighed and homogenized in cold methanol containing internal standards. Briefly, lipids were extracted with chloroform (2 vol) and washed with water (1 vol). Organic phases were collected and dried under liquid nitrogen. Lipids were reconstituted in chloroform/methanol (1:4, ν/ν) for liquid chromatography/mass spectrometry (LC/MS) analyses. Lipid identification and quantification are described below.

Lipid Analyses: Free Fatty Acids (FAs)—To analyze FAs we used an Agilent 1100-LC system (Agilent Technologies) coupled to a 1946D-MS detector equipped with an electrospray ionization (ESI) interface (Agilent Technologies). We used a reversed-phase XDB Eclipse C_{18} column (50 $\times$ 4.6 mm i.d., 1.8 μm; Zorbax; Agilent Technologies) eluted with a linear gradient from 90 to 100% of A in B for 2.5 min at a flow rate of 1.5 ml/min with column temperature at 40 °C. Mobile phase A consisted of methanol containing 0.25% acetic acid and 5 mM ammonium acetate; mobile phase B consisted of water containing 0.25% acetic acid and 5 mM ammonium acetate. ESI was in the negative mode, capillary voltage was set at 4 kV, and fragmentor voltage was 100 V. Nitrogen was used as drying gas at a flow rate of 13 liters/min and a temperature of 350 °C. Nebulizer pressure was set at 60 psi. We used commercially available fatty acids as reference standards, monitoring deprotonated molecular ions. d_8-arachidonic acid ($m/z = 311$, Cayman Chemicals) was the internal standard. The m/z values for all the FA species are as follows: C16:0 (m/z 255), C18:0 (m/z 283), C20:0 (m/z 311), C22:0 (m/z 339), C24:0 (m/z 367), C26:0 (m/z 395), C16:1 (m/z 253), C18:1 (m/z 281), C20:1 (m/z 309), C22:1 (m/z 337), C24:1 (m/z 365), C26:1 (m/z 393), C20:3 n-9 (m/z 305), C18:2 n-6 (m/z 279), C20:3 n-6 (m/z 305), C20:4 n-6 (m/z 303), C22:4 n-6 (m/z 331), C22:5 n-6 (m/z 329), C18:3 n-3 (m/z 277), C20:5 n-3 (m/z 301), C22:5 n-3 (m/z 329), C22:6 n-3 (m/z 327).

Lipid Analyses: Cholesterol and Triacylglycerol (TAG) Species—We used an Agilent 1100-LC system coupled to a MS detector Ion-Trap XCT interfaced with atmospheric pressure chemical ionization (Agilent Technologies). Lipids were separated on a Poroshell 300 SBC18 column (2.1 $\times$ 75 mm i.d., 5 μm, Agilent Technologies) at 50 °C. A linear gradient of methanol in water containing 5 mM ammonium acetate and 0.25% acetic acid (from 85% to 100% of methanol in 4 min) was applied at a flow rate of 1 ml/min. MS detection was set in positive mode. Corona discharge needle voltage set at 4000 V. Capillary voltage was 4.0 kV, skim1 40 V, and capillary exit at 118 V. Nitrogen was used as drying gas at a flow rate of 10 liters/min, temperature of 350 °C, nebulizer pressure of 50 PSI, and vaporization temperature at 400 °C. Helium was used as collision gas.

Cholesterol was detected at m/z 369.3 as $[M+H-H_2O]^+$ at 1.8 min. Cholesterol esters were quantified after loss of the protonated cholesterol-H_2O fragment at m/z 369.3 at a selected interval of retention time (from 3.5 to 4.5 min). Total triglycerides were quantified by integrating the area of the total ion current (m/z 800–900) at a selected interval of retention time (from 4 to 5 min). TAG 19:1/19:1/19:1 (m/z 944.8, Nu-Chek Prep) was used as internal standard.

Statistical Analysis—All values are presented as mean ± S.D. Statistical significance was determined by the Student's t test. Statistical significance was assumed when *, $p < 0.05$.

Author Contributions—M. M. B. conducted most of the experiments and analyzed the results, prepared the figures and wrote the paper. S. M. performed the Q-PCR experiments shown in Fig. 4, *A* and *D* and drafted the article. G. A. performed the lipidomic experiments. PS-C, MAD-F, and GS conceived and designed the study and wrote the paper. All authors analyzed and reviewed the results and approved the final version of the manuscript.

References

1. Fausto, N., Campbell, J. S., and Riehle, K. J. (2006) Liver regeneration. *Hepatology* **43,** S45–53
2. Michalopoulos, G. K. (2007) Liver regeneration. *J. Cell. Physiol.* **213,** 286–300
3. Higgins, G. M., and Anderson, R. M. (1931) Experimental pathology of liver: restoration of liver in white rat following partial surgical removal. *Arch. Pathol.* **12,** 186–202
4. Bellet, M. M., Piobbico, D., Bartoli, D., Castelli, M., Pieroni, S., Brunacci, C., Chiacchiaretta, M., Del Sordo, R., Fallarino, F., Sidoni, A., Puccetti, P., Romani, L., Servillo, G., and Della Fazia, M. A. (2014) NEDD4 controls the expression of GUCD1, a protein upregulated in proliferating liver cells. *Cell Cycle* **13,** 1902–1911
5. Della Fazia, M. A., Castelli, M., Bartoli, D., Pieroni, S., Pettirossi, V., Piobbico, D., Viola-Magni, M., and Servillo, G. (2005) HOPS: a novel cAMP-dependent shuttling protein involved in protein synthesis regulation. *J. Cell Sci.* **118,** 3185–3194
6. Della Fazia, M. A., Pettirossi, V., Ayroldi, E., Riccardi, C., Magni, M. V., and Servillo, G. (2001) Differential expression of CD44 isoforms during liver regeneration in rats. *J. Hepatol.* **34,** 555–561
7. Servillo, G., Della Fazia, M. A., and Sassone-Corsi, P. (1998) Transcription factor CREM coordinates the timing of hepatocyte proliferation in the regenerating liver. *Genes Dev.* **12,** 3639–3643
8. Servillo, G., Della Fazia, M. A., and Sassone-Corsi, P. (2002) Coupling cAMP signaling to transcription in the liver: pivotal role of CREB and CREM. *Exp. Cell Res.* **275,** 143–154
9. Bartoli, D., Piobbico, D., Bellet, M. M., Bennati, A. M., Roberti, R., Della Fazia, M. A., and Servillo, G. (2016) Impaired cell proliferation in regenerating liver of 3β-hydroxysterol δ14-reductase (TM7SF2) knock-out mice. *Cell Cycle* 1–10
10. Farrell, G. C. (2004) Probing Prometheus: fat fueling the fire? *Hepatology* **40,** 1252–1255
11. Guarente, L. (2011) Sirtuins, aging, and metabolism. *Cold Spring Harb. Symp. Quant. Biol.* **76,** 81–90
12. Finkel, T., Deng, C. X., and Mostoslavsky, R. (2009) Recent progress in the biology and physiology of sirtuins. *Nature* **460,** 587–591
13. Asher, G., Gatfield, D., Stratmann, M., Reinke, H., Dibner, C., Kreppel, F., Mostoslavsky, R., Alt, F. W., and Schibler, U. (2008) SIRT1 regulates circadian clock gene expression through PER2 deacetylation. *Cell* **134,** 317–328
14. Chang, H. C., and Guarente, L. (2013) SIRT1 mediates central circadian control in the SCN by a mechanism that decays with aging. *Cell* **153,** 1448–1460
15. Nakahata, Y., Kaluzova, M., Grimaldi, B., Sahar, S., Hirayama, J., Chen, D., Guarente, L. P., and Sassone-Corsi, P. (2008) The NAD+-dependent deacetylase SIRT1 modulates CLOCK-mediated chromatin remodeling and circadian control. *Cell* **134,** 329–340
16. Nakahata, Y., Sahar, S., Astarita, G., Kaluzova, M., and Sassone-Corsi, P. (2009) Circadian control of the NAD+ salvage pathway by CLOCK-SIRT1. *Science* **324,** 654–657
17. Ramsey, K. M., Yoshino, J., Brace, C. S., Abrassart, D., Kobayashi, Y., Marcheva, B., Hong, H. K., Chong, J. L., Buhr, E. D., Lee, C., Takahashi, J. S., Imai, S., and Bass, J. (2009) Circadian clock feedback cycle through NAMPT-mediated NAD+ biosynthesis. *Science* **324,** 651–654
18. Bellet, M. M., Nakahata, Y., Boudjelal, M., Watts, E., Mossakowska, D. E., Edwards, K. A., Cervantes, M., Astarita, G., Loh, C., Ellis, J. L., Vlasuk, G. P., and Sassone-Corsi, P. (2013) Pharmacological modulation of circadian rhythms by synthetic activators of the deacetylase SIRT1. *Proc. Natl. Acad. Sci. U.S.A.* **110,** 3333–3338
19. Masri, S., Rigor, P., Cervantes, M., Ceglia, N., Sebastian, C., Xiao, C., Roqueta-Rivera, M., Deng, C., Osborne, T. F., Mostoslavsky, R., Baldi, P., and Sassone-Corsi, P. (2014) Partitioning circadian transcription by SIRT6 leads to segregated control of cellular metabolism. *Cell* **158,** 659–672
20. Sahar, S., and Sassone-Corsi, P. (2009) Metabolism and cancer: the circadian clock connection. *Nat. Rev. Cancer* **9,** 886–896
21. Fu, L., Pelicano, H., Liu, J., Huang, P., and Lee, C. (2002) The circadian gene Period2 plays an important role in tumor suppression and DNA damage response *in vivo*. *Cell* **111,** 41–50
22. Gery, S., Komatsu, N., Baldjyan, L., Yu, A., Koo, D., and Koeffler, H. P. (2006) The circadian gene per1 plays an important role in cell growth and DNA damage control in human cancer cells. *Mol. Cell* **22,** 375–382
23. Kang, T. H., Reardon, J. T., Kemp, M., and Sancar, A. (2009) Circadian oscillation of nucleotide excision repair in mammalian brain. *Proc. Natl. Acad. Sci. U.S.A.* **106,** 2864–2867
24. Matsuo, T., Yamaguchi, S., Mitsui, S., Emi, A., Shimoda, F., and Okamura, H. (2003) Control mechanism of the circadian clock for timing of cell division in vivo. *Science* **302,** 255–259
25. Albrecht, J. H., Poon, R. Y., Ahonen, C. L., Rieland, B. M., Deng, C., and Crary, G. S. (1998) Involvement of p21 and p27 in the regulation of CDK activity and cell cycle progression in the regenerating liver. *Oncogene* **16,** 2141–2150
26. Aguilar-Arnal, L., Katada, S., Orozco-Solis, R., and Sassone-Corsi, P. (2015) NAD(+)-SIRT1 control of H3K4 trimethylation through circadian deacetylation of MLL1. *Nat. Struct. Mol. Biol.* **22,** 312–318
27. Rudnick, D. A., and Davidson, N. O. (2012) Functional relationships between lipid metabolism and liver regeneration. *Int. J. Hepatol.* :549241, 2012
28. Purushotham, A., Schug, T. T., Xu, Q., Surapureddi, S., Guo, X., and Li, X. (2009) Hepatocyte-specific deletion of SIRT1 alters fatty acid metabolism and results in hepatic steatosis and inflammation. *Cell Metab.* **9,** 327–338
29. Chen, D., Bruno, J., Easlon, E., Lin, S. J., Cheng, H. L., Alt, F. W., and Guarente, L. (2008) Tissue-specific regulation of SIRT1 by calorie restriction. *Genes Dev.* **22,** 1753–1757
30. Ponugoti, B., Kim, D. H., Xiao, Z., Smith, Z., Miao, J., Zang, M., Wu, S. Y., Chiang, C. M., Veenstra, T. D., and Kemper, J. K. (2010) SIRT1 deacetylates and inhibits SREBP-1C activity in regulation of hepatic lipid metabolism. *J. Biol. Chem.* **285,** 33959–33970
31. Schmutz, I., Ripperger, J. A., Baeriswyl-Aebischer, S., and Albrecht, U. (2010) The mammalian clock component PERIOD2 coordinates circadian output by interaction with nuclear receptors. *Genes Dev.* **24,** 345–357
32. Jin, J., Iakova, P., Jiang, Y., Medrano, E. E., and Timchenko, N. A. (2011) The reduction of SIRT1 in livers of old mice leads to impaired body

homeostasis and to inhibition of liver proliferation. *Hepatology* **54,** 989 –998

33. García-Rodríguez, J. L., Barbier-Torres, L., Fernández-Álvarez, S., Gutiérrez-de Juan, V., Monte, M. J., Halilbasic, E., Herranz, D., Álvarez, L., Aspichueta, P., Marín, J. J., Trauner, M., Mato, J. M., Serrano, M., Beraza, N., and Martínez-Chantar, M. L. (2014) SIRT1 controls liver regeneration by regulating bile acid metabolism through farnesoid X receptor and mammalian target of rapamycin signaling. *Hepatology* **59,** 1972–1983

34. Cheng, H. L., Mostoslavsky, R., Saito, S., Manis, J. P., Gu, Y., Patel, P., Bronson, R., Appella, E., Alt, F. W., and Chua, K. F. (2003) Developmental defects and p53 hyperacetylation in Sir2 homolog (SIRT1)-deficient mice. *Proc. Natl. Acad. Sci. U.S.A.* **100,** 10794–10799

35. Shteyer, E., Liao, Y., Muglia, L. J., Hruz, P. W., and Rudnick, D. A. (2004) Disruption of hepatic adipogenesis is associated with impaired liver regeneration in mice. *Hepatology* **40,** 1322–1332

36. Abel, S., Smuts, C. M., de Villiers, C., and Gelderblom, W. C. (2001) Changes in essential fatty acid patterns associated with normal liver regeneration and the progression of hepatocyte nodules in rat hepatocarcinogenesis. *Carcinogenesis* **22,** 795–804

37. Anderson, S. P., Yoon, L., Richard, E. B., Dunn, C. S., Cattley, R. C., and Corton, J. C. (2002) Delayed liver regeneration in peroxisome proliferator-activated receptor-α-null mice. *Hepatology* **36,** 544–554

38. Hallows, W. C., Lee, S., and Denu, J. M. (2006) Sirtuins deacetylate and activate mammalian acetyl-CoA synthetases. *Proc. Natl. Acad. Sci. U.S.A.* **103,** 10230–10235

39. Sahar, S., Masubuchi, S., Eckel-Mahan, K., Vollmer, S., Galla, L., Ceglia, N., Masri, S., Barth, T. K., Grimaldi, B., Oluyemi, O., Astarita, G., Hallows, W. C., Piomelli, D., Imhof, A., Baldi, P., Denu, J. M., and Sassone-Corsi, P. (2014) Circadian control of fatty acid elongation by SIRT1 protein-mediated deacetylation of acetyl-coenzyme A synthetase 1. *J. Biol. Chem.* **289,** 6091–6097